

## Sorafenib Inhibits Cell Migration and Stroma-Mediated Bortezomib Resistance by Interfering B-cell Receptor Signaling and Protein Translation in Mantle Cell Lymphoma

Sílvia Xargay-Torrent, Mónica López-Guerra, Arnau Montraveta, Ifigènia Saborit-Villarroya, Laia Rosich, Alba Navarro, Patricia Pérez-Galán, Gaël Roué, Elias Campo, and Dolors Colomer

### Abstract

**Purpose:** We evaluated the antitumoral properties of the multikinase inhibitor sorafenib in mantle cell lymphoma (MCL), an aggressive B lymphoma for which current therapies have shown limited efficacy.

**Experimental Design:** Sensitivity to sorafenib was analyzed in MCL cell lines and primary samples in the context of BCR and microenvironment simulation. Sorafenib signaling was characterized by quantitative PCR, Western blotting, immunofluorescence, and protein immunoprecipitation. Migration analysis included flow cytometric counting, actin polymerization assays, and siRNA-mediated knockdown of focal adhesion kinase (FAK). *In vivo* antitumor effect of sorafenib and bortezomib was analyzed in an MCL xenograft mouse model.

**Results:** Sorafenib rapidly dephosphorylates the BCR-associated kinases, Syk and Lyn, as well as FAK, an Src target involved in focal adhesion. In this line, sorafenib displays strong synergy with the Syk inhibitor, R406. Sorafenib also blocks Mcl-1 and cyclin D1 translation, which promotes an imbalance between pro- and antiapoptotic proteins and facilitates Bax release from cyclin D1, leading to the induction of mitochondrial apoptosis and caspase-dependent and -independent mechanisms. Moreover, sorafenib inhibits MCL cell migration and CXCL12-induced actin polymerization. FAK knockdown partially prevents this inhibitory effect, indicating that FAK is a relevant target of sorafenib. Furthermore, sorafenib enhances the antitumoral activity of bortezomib in an MCL xenograft mouse model as well as overcomes stroma-mediated bortezomib resistance in MCL cells.

**Conclusion:** We show for the first time that sorafenib interferes with BCR signaling, protein translation and modulates the microenvironment prosurvival signals in MCL, suggesting that sorafenib, alone or in combination with bortezomib, may represent a promising approach to treat patients with MCL. *Clin Cancer Res*; 19(3); 586–97. ©2012 AACR.

### Introduction

Mantle cell lymphoma (MCL) is an incurable B-cell neoplasm harboring the t(11;14)(q13;q32) translocation, which leads to the overexpression of cyclin D1 with the consequent cell-cycle deregulation (1). Typically, MCL is characterized by relatively short survival and brief responses to conventional chemotherapy (2). Thus, new preclinical studies on innovative therapeutic strategies are warranted. In this context, the constitutive acti-

vation of several signaling pathways regulated by kinases has been described in MCL cells (3), opening up a new horizon in the treatment of this entity. Specifically, new targeted agents that interfere with B-cell receptor (BCR) signaling, such as Syk, Btk, and phosphoinositide 3-kinase (PI3K) inhibitors, are entering clinical trials. Although the number of patients with MCLs treated with these agents is still very low, preliminary data seem to indicate that the responses to the Btk inhibitor PCI-32765 and the PI3K inhibitor CAL-101 are very favorable (4, 5). In B lymphocytes, activation of the BCR by antigen engagement induces the phosphorylation of Src family kinases, for instance, Lyn, leading to the recruitment of Syk. Once phosphorylated, Lyn and Syk propagate the BCR signal by activating downstream kinases, such as Btk, resulting in the activation of multiple downstream signaling pathways. Recently, it has been reported that MCL cells have constitutive activation of the BCR signal transduction proteins Syk and PKC $\beta$ II (6, 7), as well as high expression of the phosphorylated forms of these and other BCR-associated kinases (8).

**Authors' Affiliation:** Hematopathology Unit, Department of Pathology, Hospital Clínic, Institut d'Investigacions Biomèdiques August Pi i Sunyer (IDIBAPS), University of Barcelona, Barcelona, Spain

**Note:** S. Xargay-Torrent and M. López-Guerra contributed equally to this work.

**Corresponding Author:** Dolors Colomer, Hematopathology Unit, Hospital Clínic, Villarroel 170, Barcelona 08036, Spain. Phone/Fax: 34-932275572; Fax: 34-932275572; E-mail: dcolomer@clinic.cat

**doi:** 10.1158/1078-0432.CCR-12-1935

©2012 American Association for Cancer Research.

### Translational Relevance

Mantle cell lymphoma (MCL) is a B lymphoid neoplasm with short survival and brief responses to current therapies, thus novel therapeutic strategies are needed. The constitutive activation of several signaling pathways regulated by kinases has been described in MCL cells, in particular those related with B-cell receptor (BCR) signaling. Sorafenib is an approved multikinase inhibitor currently in clinical trials for several hematologic malignancies. In this work, we show for first time the antitumoral properties of sorafenib in MCL. Our results provide a novel mechanism of action of this compound in MCL cells, establishing that sorafenib interferes with BCR signaling, protein translation and modulates the migratory and microenvironmental prosurvival signals in MCL. These results suggest that sorafenib alone or in combination with bortezomib-based therapies may represent a promising approach to treat patients with MCL and hopefully meet a medical need.

On the other hand, the crosstalk between tumor MCL cells and stroma in tissue microenvironments, such as bone marrow and secondary lymphoid tissues, has also been found to play an important role in the biology of the disease. *In vitro* studies showed that MCL cells interact with bone marrow stromal cells, becoming resistant to conventional cytotoxic agents (9). New therapeutic strategies directed to disrupt these interactions include targeting signaling kinases (such as Lyn, Syk, Btk, and PI3K) as well as adhesion molecules and chemokine receptors, which have also been found to be highly expressed in MCL (10). BCR activation also regulates the signaling of these receptors modulating B-cell trafficking and tissue homing. Accordingly, targets downstream Src activation include focal adhesion kinase (FAK) that promotes invasiveness and may act as a link between BCR signaling and migration/adhesion through the actin cytoskeleton (11, 12).

Sorafenib (BAY 43-9006) is a multikinase inhibitor that has been approved for the treatment of advanced renal cell carcinoma (13) and hepatocellular carcinoma (14). Currently, there are several clinical trials in hematologic malignancies, first in chronic myeloid leukemia and acute myeloid leukemia, where sorafenib targets BCR-ABL (15) and FLT3 (16) oncogenic kinases, and more recently in chronic lymphocytic leukemia (CLL; Identifier: NCT01510756). Further *in vitro* studies have shown that leukemic cells are susceptible to this agent (17, 18), its cytotoxic effect being related to the translational inhibition of the antiapoptotic protein Mcl-1 (17, 19). Recently, we have proposed that in CLL cells, sorafenib overcomes microenvironmental signals and abrogates BCR-derived responses (20).

The antitumor activity and the molecular mechanism of action of sorafenib in MCL have not been yet elucidated;

therefore, the aim of this study was to characterize the molecular mechanisms underlying sorafenib-induced apoptosis in MCL cells, with particular emphasis on BCR signaling and protein translation. We further investigated the efficacy of sorafenib in modulating migratory and microenvironmental prosurvival signals in MCL, both alone and in combination with bortezomib.

### Materials and Methods

#### Cell lines

Nine human MCL cell lines (GRANTA-519, HBL-2, REC-1, JEKO-1, MINO, JVM-2, Z-138, UPN-1, and MAVER-1), which were genetically characterized previously (21), were used (Table 1). Cell lines were grown in RPMI-1640 or Dulbecco's modified Eagle's medium (DMEM) supplemented with 10% to 20% heat-inactivated FBS, 2 mmol/L glutamine, 50 µg/mL penicillin-streptomycin (Life Technologies) and maintained in a humidified atmosphere at 37°C with 5% carbon dioxide. Mycoplasma absence was routinely tested by PCR, and the genetic identity of all cell lines was verified by using AmpFISTR identifier kit (Life Technologies).

#### Isolation and culture of primary cells

Tumor cells from 17 patients diagnosed of MCL, according to the World Health Organization classification criteria (22), were used. The Ethical Committee of the Hospital Clínic (Barcelona, Spain) authorized the study, and all patients signed an informed consent according to the Declaration of Helsinki. The characteristics of these cases are listed in Table 1. Tumor cells from peripheral blood were isolated by density gradient centrifugation using Ficoll-Paque (GE Healthcare), whereas counterparts from tumor tissue were obtained after squirting with RPMI using a fine needle. Samples were cryopreserved in liquid nitrogen in the presence of 10% dimethyl sulfoxide (Sigma), 60% FBS, and 30% RPMI and conserved within the Hematopathology collection of our institution (IDIBAPS-Hospital Clínic Biobank). Freezing/thawing manipulations did not influence cell response (23). Cells were cultured in supplemented RPMI medium likewise cell lines. The immunoglobulin heavy chain variable (*IGHV*) gene mutational status was done according to European Research Initiative on CLL (ERIC) guidelines (24). Cytogenetic alterations were assessed by FISH. In cases with 17p deletions, the mutational analysis of the second allele was done by direct sequencing according to the International Agency for Research on Cancer (IARC) TP53 consortium (<http://p53.iarc.fr>).

#### Drugs and assessment of apoptotic features by flow cytometry

MCL samples were treated as indicated with sorafenib (Bayer), R406 (Selleck Chemicals), and/or bortezomib (Millennium Pharmaceuticals). When specified, cells were either preincubated for 1 hour with 10 µmol/L of the pan-caspase inhibitor Q-VD-OPH (Calbiochem) or exposed to

**Table 1.** MCL cell lines and primary samples characteristics

MCL cell line	Sorafenib LD <sub>50</sub> 24 h, $\mu\text{mol/L}$	Sorafenib LD <sub>50</sub> 48 h, $\mu\text{mol/L}$	p53 <sup>a</sup>	ATM	P16	% IGHV homology <sup>b</sup>
GRANTA-519	19.8	13.0	del/wt	del/mut	hom del	100
HBL-2	15.6	7.2	del/mut	upd/ <sup>c</sup>	hom del	97.57
REC-1	14.5	5.8	wt/mut	wt/ <sup>c</sup>	hom del	98.61
JEKO-1	13.5	9.1	del/mut	ampl/ <sup>c</sup>	del/ <sup>c</sup>	99.66
MINO	12.4	6.4	upd/mut	wt/ <sup>c</sup>	upd/ <sup>c</sup>	ND
JVM-2	10.4	7.8	wt	wt	wt/ <sup>c</sup>	100
Z-138	6.8	5.6	wt	del/ <sup>c</sup>	hom del	98.96
UPN-1	5.3	4.3	del/mut	wt/polimorf	del/ <sup>c</sup>	100
MAVER-1	5.2	4.8	del/mut	del/ <sup>c</sup>	hom del	100

MCL patient	Sorafenib LD <sub>50</sub> 24 h, $\mu\text{mol/L}$	Sorafenib LD <sub>50</sub> 48 h, $\mu\text{mol/L}$	Disease status	Cell source	% of tumor cells <sup>d</sup>	p53 <sup>a</sup>	% IGHV homology <sup>b</sup>
MCL#1	NR	10.4	Diagnosis	PB	96	del/wt	93.18
MCL#2	11.1	7.7	Diagnosis	PB	97	wt	92.36
MCL#3	16.2	15.5	Diagnosis	PB	83	wt	97.92
MCL#4	9.9	6.1	Diagnosis	PB	86	wt	99.65
MCL#5	13.3	9.2	Diagnosis	PB	85	wt	98.61
MCL#6	14.1	12.0	Diagnosis	PB	92	wt	ND
MCL#7	7.5	5.8	Diagnosis	PB	94	wt	96.88
MCL#8	5.1	2.0	Relapse	PB	95	del/mut	98.25
MCL#9	11.6	9.5	ND	PB	84	wt	96.9
MCL#10	18.1	12.4	Diagnosis	PB	79	del/wt	94.44
MCL#11	13.2	10.0	Diagnosis	PB	96	del/mut	97.22
MCL#12	NR	ND	Diagnosis	PB	83	wt	93.68
MCL#13	11.6	11.4	Diagnosis	PB	77	wt	96.89
MCL#14	NR	ND	Diagnosis	PB	71	wt	100
MCL#14	14.8	ND	Diagnosis	LN	89	wt	100
MCL#15	15.9	ND	Diagnosis	LN	78	wt	99.65
MCL#16	16.6	10.6	Relapse	Orbit	88	ND	95.83
MCL#17	15.4	ND	Diagnosis	LN	82	wt	96.65

Abbreviations: ampl, amplification; del, deletion; hom del, homozygous deletion; ND, not determined; NR, not reached; LN, lymph node; mut, mutation; PB, peripheral blood; upd, uniparental disomy; wt, wild-type.

<sup>a</sup>p53 mutational status detected by FISH and direct sequencing.

<sup>b</sup>IGHV gene mutational status was done according to standardized protocols (24).

<sup>c</sup>Mutations not analyzed.

<sup>d</sup>CD19<sup>+</sup> tumor cells quantified by flow cytometry.

100  $\mu\text{mol/L}$  of the translation inhibitor cycloheximide (Sigma) for 1 hour after 4 hours of sorafenib. Apoptosis was quantified by double labeling of phosphatidylserine (PS) exposure with Annexin V-fluorescein isothiocyanate (FITC) and nuclei with propidium iodide (PI; Bender Med-systems). Loss of mitochondrial membrane potential ( $\Delta\psi\text{m}$ ), caspase-3 activation, and Bax and Bak conformational changes were determined as previously described (25). Lethal dose 50 (LD<sub>50</sub>) was defined as the concentration of drug required to reduce cell viability by 50%. For drug combination studies, combination indexes (CI) were calculated with the CalcuSyn software version 2.0

(Biosoft) according to the Chou and Talalay algorithm. The interaction between 2 drugs was considered synergistic when CI < 1.

#### BCR stimulation

Primary MCL cells were washed twice and starved for 1.5 hours in FBS-free RPMI (10<sup>7</sup> cells/mL). Then, cells were reacted for 30 minutes at 4°C with 25  $\mu\text{g/mL}$  of anti-IgM (Jackson Immunoresearch Laboratories) and subsequently transferred to 37°C for 30 additional minutes. When indicated, cells were preincubated with sorafenib for 1.5 hours before anti-IgM addition.

### Immunoprecipitation, subcellular fractionation, and Western blot analysis

Whole protein extraction and Western blot analysis were done as described previously (26). For cyclin D1 immunoprecipitation, cells were lysed in CHAPS buffer (1% CHAPS, 100 mmol/L NaCl, 5 mmol/L Na<sub>2</sub>HPO<sub>4</sub>, and 2.5 mmol/L EDTA) supplemented as follows: 1 mmol/L phenylmethanesulfonyl fluoride, 2 mmol/L sodium pyrophosphate decahydrate, 2 mmol/L sodium β-glycerophosphate, 1 mmol/L Na<sub>3</sub>VO<sub>4</sub>, 10 μg/mL aprotinin, and 10 μg/mL leupeptin (Sigma). Extracts were precleared with A-protein agarose beads (Calbiochem) for 30 minutes, incubated overnight at 4°C with cyclin D1 (DCS6; Cell Signaling Technology) antibody, and immunoprecipitated for 1 hour with A-protein beads. Supernatant (unbound fraction) was recovered by centrifugation, and beads (bound fraction) were washed 3 times with lysis buffer. For subcellular fractionation, cytosolic and mitochondrial fractions were obtained with the ApoAlert Cell Fractionation Kit (Clontech) according to manufacturer's instructions. The following primary antibodies were used: pSyk (Tyr352), pLyn (Tyr396), pFAK (Tyr397), cyclin D1 (DCS6), pelf4E (Ser209) from Cell Signaling Technology; AIF from Sigma; and Mcl-1 and Bax (N-20) from Santa Cruz. Equal protein loading was confirmed by probing membranes with β-actin and β-tubulin antibodies (Sigma). Densitometric quantification was done by using Image Gauge software (Fujifilm).

### mRNA quantification by real-time PCR

Total RNA isolation and retrotranscription to cDNA were done as previously reported (25). *CYCLIN D1* and *MCL-1* expression was analyzed in duplicate with pre-designed Assay-On-Demand probes (Life Technologies) on a StepOne device (Life Technologies) by quantitative real-time PCR (qRT-PCR). The relative expression of each gene was quantified by the comparative cycle threshold (C<sub>t</sub>) method (ΔΔC<sub>t</sub>) by using β-glucuronidase (*GUSB*; Life Technologies) as endogenous control. Expression levels are given in arbitrary units, taking as a reference the control sample (untreated cells).

### Immunofluorescence

One million of primary cells were attached on poly-L-lysine-coated glass coverslips, fixed with 4% paraformaldehyde, and permeabilized with 0.1% saponin and 10% FBS in PBS. Samples were then incubated with anti-AIF antibody (Sigma) followed by anti-rabbit-FITC secondary antibody (Sigma). Coverslips were mounted on glass slides with Fluoroshield with DAPI (4',6 diamidino-2-phenylindole) medium (Sigma) and visualized on a Eclipse 50i microscope (Nikon) by means of a 100×/1.30 numerical aperture (NA) oil objective (Nikon) using the Isis Imaging System v5.3 software (MetaSystems GmbH).

### Chemotaxis assay

MCL cells (10<sup>7</sup> cells/mL) were washed twice and serum-starved for 1.5 hours in FBS-free RPMI. Sorafenib was added for 1.5 additional hours, and cells were diluted to

× 10<sup>6</sup> cells/mL with 0.5% bovine serum albumin (BSA; Sigma) in RPMI. One hundred microliters (5 × 10<sup>5</sup> cells) was added to the top chamber of a Transwell culture polycarbonate insert with 6.5-mm diameter and 5 μm of pore size (Corning). Inserts had been previously transferred to wells containing 600 μL of RPMI with or without 200 ng/mL of human recombinant CXCL12 (Peprotech). After 4 hours of incubation at 37°C, 100 μL was collected in triplicate from each lower chamber and counted by flow cytometry (FACScan) for 1 minute under constant flow rate.

### siRNA assay

Five million cells were cultured without antibiotics and washed with FBS-free RPMI. Then, cells were resuspended in 100 μL of Ingenio Electroporation Solution (Mirus) containing either 5 μmol/L of FAK Silencer Select Pre-designed siRNA (Life Technologies) or 5 μmol/L of a non-silencing negative control (Life Technologies). Cells were transfected in a Nucleofector II device (Lonza) by using M-013 program, transferred to culture plates overnight, and chemotaxis assay was conducted as described above.

### Actin polymerization

MCL cells (10<sup>7</sup> cells/mL) were washed twice and serum-starved for 1.5 hours in FBS-free RPMI. Sorafenib or the CXCR4 antagonist AMD3100 (40 μmol/L; Sigma) were added for 1.5 additional hours, and cells were diluted to 0.7 × 10<sup>6</sup> or 2 × 10<sup>6</sup> cells/mL in RPMI with 0.5% BSA for cell lines and primary cells respectively. Thereafter, samples were stimulated with 200 ng/mL of CXCL12 and at the indicated time points, 400 μL of the cell suspension was collected and added to 100 μL of the staining solution [2.5 or 12.5 ng/mL of phalloidin-Tetramethyl Rhodamine Isothiocyanate (TRITC) for primary cells and cell lines, respectively, 2.5 mg/mL of L-α-lysophosphatidylcholine (Sigma) and 5% paraformaldehyde (Anamed)] for 20 minutes at 37°C. Red fluorescence was acquired on an Attune acoustic cytometer (Life Technologies), and results were plotted relative to the mean fluorescence of the sample before the addition of CXCL12.

### Stroma coculture

Human follicular dendritic cell-like HK (kindly provided by Dr. Y.S. Choi; ref. 27) and human bone marrow-derived stroma cell line HS-5 (American Type Culture Collection) were cultured in Iscove's modified Dulbecco's medium (IMDM) and DMEM, respectively, and supplemented as above. Before setting up the experiment, HK (1 × 10<sup>5</sup> cells/mL) and HS-5 cells (2 × 10<sup>5</sup> cells/mL) were plated overnight, and after confirming the confluence of the stroma layer, medium was replaced by 5 × 10<sup>5</sup> MCL primary cells in RPMI, and cells were incubated at 37°C for 2 hours before adding the drugs. Sorafenib was preincubated for 1 hour before bortezomib addition. Afterward, MCL cells were collected by carefully rinsing the wells without disturbing the stroma monolayer.

### Xenograft mouse model

Six-week-old CB17-severe combined immunodeficient female mice (SCID; Charles River) were inoculated subcutaneously into the right flank with 1:1 of  $10^7$  Jeko-1 cells in PBS and Matrigel basement membrane matrix (Becton Dickinson), according to a protocol approved by the animal testing ethical committee of the University of Barcelona (Barcelona, Spain). When tumors were palpable, mice were randomly assigned into 4 cohorts of 4 each. Sorafenib (80 mg/kg) or vehicle were administered by oral gavage 5 d/wk, formulated in 50% cremophor EL (Sigma) and 50% of ethanol 95% (Panreac), which was diluted 1:4 with distilled water right before administration. Bortezomib (0.3 mg/kg) or PBS vehicle were given twice a week through intraperitoneal injection. Tumor volumes were calculated according to the formula: (the shortest diameter)<sup>2</sup> × (the longest diameter) × 0.5.

### Statistical analysis

The data are depicted as the mean ± SD of 3 independent experiments or the mean ± SEM of 4 or more cases. All statistical analyses were done by using GraphPad Prism 4.0 software (GraphPad Software). Comparison of means between 2 groups of samples was evaluated by nonparametric Mann-Whitney test or paired *t* test. Results were considered statistically significant when  $P < 0.05$  (\*,  $P < 0.05$ ; \*\*,  $P < 0.01$ ).

## Results

### Sorafenib induces apoptosis in MCL cells

The cytotoxicity of the multikinase inhibitor sorafenib was measured after 24 and 48 hours by Annexin V labeling in 9 MCL cell lines, incubated at doses ranging from 2.5 to 20  $\mu\text{mol/L}$ . The LD<sub>50</sub> for these MCL cell lines are listed in Table 1. Sorafenib induced apoptosis in all of them, with a mean LD<sub>50</sub> of  $11.5 \pm 5.0$   $\mu\text{mol/L}$  at 24 hours, whereas at 48 hours decreased to  $7.1 \pm 2.7$   $\mu\text{mol/L}$ . No association was observed between sorafenib sensitivity and any of the most frequent genetic alterations in MCL, nor the mutational status of *IGHV*. For subsequent analysis, Jeko-1 and Z-138 cell lines were selected as representative cell lines, with LD<sub>50</sub> of 13.5 and 6.8  $\mu\text{mol/L}$  at 24 hours, respectively.

Primary cells from 17 patients diagnosed of MCL were also incubated with increasing doses of sorafenib for 24 and 48 hours. The characteristics of these patients are summarized in Table 1. Despite the high variability among cases, the mean LD<sub>50</sub> was  $13.0 \pm 3.6$   $\mu\text{mol/L}$  at 24 hours, whereas at 48 hours, it notably decreased to  $9.4 \pm 3.4$   $\mu\text{mol/L}$ , thus resembling the data obtained for cell lines. Noteworthy, sorafenib was as effective in tumor cells from peripheral blood (PB) as in those derived from tumor tissue (at 24 hours mean LD<sub>50</sub> PB:  $11.8 \pm 4.0$   $\mu\text{mol/L}$ ; mean LD<sub>50</sub> tumor tissue:  $15.7 \pm 0.7$   $\mu\text{mol/L}$ ; Table 1). Similar to MCL cell lines, sensitivity to sorafenib was independent of mutational status of *P53* and *IGHV*. Importantly, LD<sub>50</sub> values were physiologically achievable and nontoxic for healthy B lymphocytes (20). Collectively, these data indicate that sorafenib exerts a time- and dose-dependent cytotoxic effect in MCL cells.

phocytes (20). Collectively, these data indicate that sorafenib exerts a time- and dose-dependent cytotoxic effect in MCL cells.

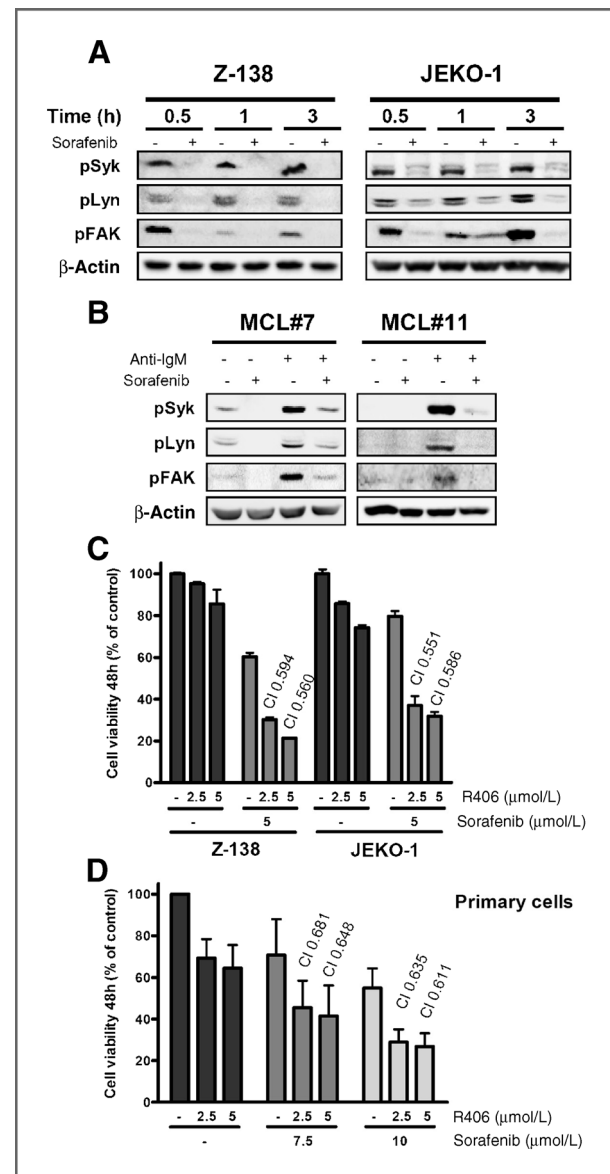


**Figure 1.** Sorafenib inhibition of BCR kinases and FAK. A, Z-138 and Jeko-1 cells were exposed to 10  $\mu\text{mol/L}$  of sorafenib for the indicated times. Phosphorylation levels of Syk, Lyn, and FAK were analyzed by Western blotting. B, cells from 2 representative patients with MCL were preincubated with 10  $\mu\text{mol/L}$  of sorafenib before anti-IgM (25  $\mu\text{g/mL}$ ) reaction. Phosphorylation of Syk, Lyn, and FAK was assessed by Western blotting. C, Z-138 and Jeko-1 cells were simultaneously exposed to sorafenib and R406 at the indicated doses, and cell viability was determined at 48 hours by Annexin V/PI staining. Bars represent the mean ± SD of 3 independent experiments. CI value is indicated for each combination. D, primary MCL cells from 7 patients were simultaneously exposed to sorafenib and R406 at the indicated doses for 48 hours, and cell viability was determined as above. Bars represent the mean ± SEM of all the samples analyzed. CI value is indicated for each combination.

### Sorafenib targets BCR kinases and FAK in MCL cells

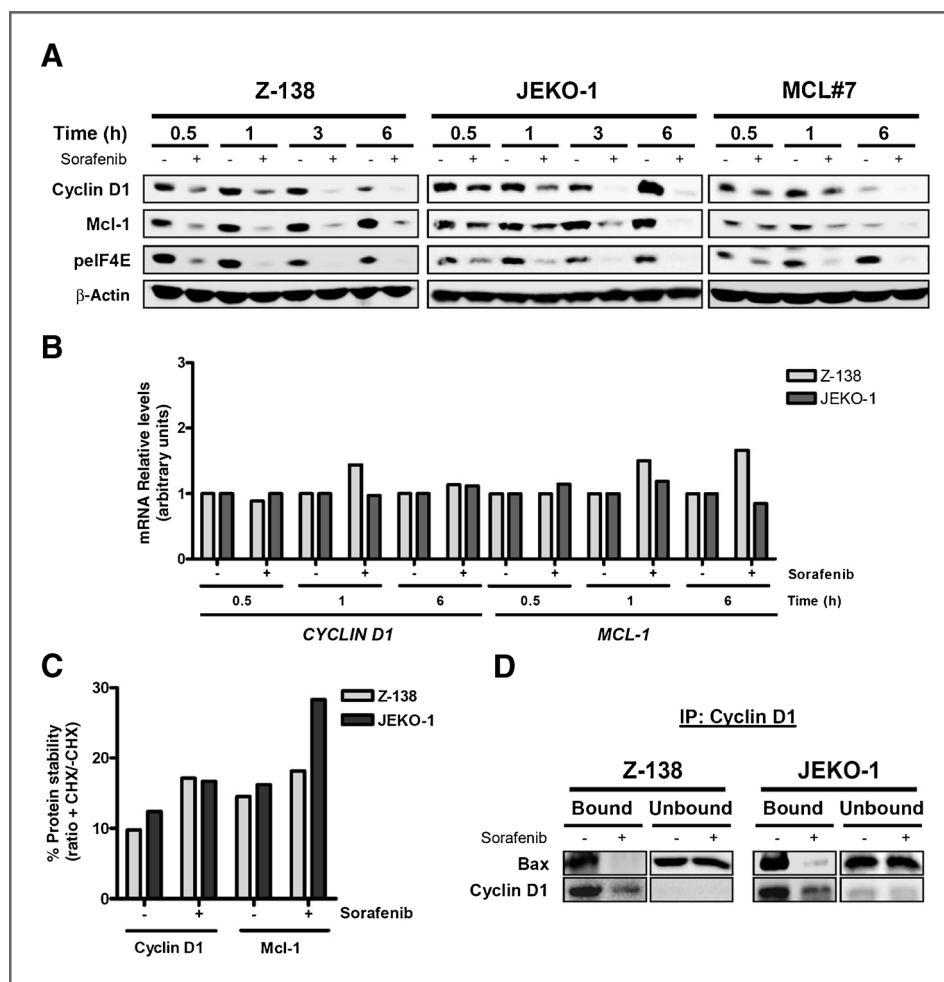
We have recently shown that sorafenib abrogates BCR-derived responses including FAK activation in CLL (20). To explore if this effect was also applicable to MCL cells, we monitored the activation of BCR-related kinases, Syk, Lyn, and FAK, by Western blotting. In Z-138 and JEKO-1 cell lines, we found that 10  $\mu\text{mol/L}$  sorafenib induced a rapid and sustained dephosphorylation of Syk, Lyn, and FAK, detectable after 30 minutes of treatment (Fig. 1A). To further confirm the effect of sorafenib on BCR signaling, primary MCL cells from 2 representative cases were stimulated with anti-IgM in the presence of sorafenib. As shown in Fig. 1B, sorafenib inhibited very efficiently the phosphorylation of Syk, Lyn, and FAK, both constitutive and induced after BCR engagement. In parallel, we investigated whether the sensitivity of MCL cells to a pharmacologic BCR inhibitor, the Syk inhibitor R406, could be enhanced by sorafenib. JEKO-1 and Z-138 cells were cotreated with low doses of sorafenib (5  $\mu\text{mol/L}$ ) and R406 (2.5 and 5  $\mu\text{mol/L}$ ) for 48 hours and cell viability was analyzed. The combination was found to be considerably more potent than each agent alone in both cell lines, with CI values of 0.594 and 0.560 for the combination of 5  $\mu\text{mol/L}$  sorafenib with 2.5 and 5  $\mu\text{mol/L}$

R406, respectively, for Z-138, and 0.551 and 0.586 for JEKO-1 (Fig. 1C). Importantly, this effect was also found in primary MCL cells, where combination of sorafenib (7.5 and 10  $\mu\text{mol/L}$ ) with R406 (2.5 and 5  $\mu\text{mol/L}$ ) revealed a strong synergy in all the samples studied ( $n = 7$ ), with a mean CI of 0.681 and 0.648 for the combination of 7.5  $\mu\text{mol/L}$  sorafenib with 2.5 and 5  $\mu\text{mol/L}$  R406, respectively, and 0.635 and 0.611 with 10  $\mu\text{mol/L}$  sorafenib (Fig. 1D). Taken together, these results suggest that sorafenib targets both constitutive and induced BCR signaling in MCL cells and enhances the activity of the Syk inhibitor R406.

### Sorafenib inhibits translation of cyclin D1 and Mcl-1 in MCL cells

As oncogenic activation of cyclin D1 is a typical hallmark of MCL, we investigated whether sorafenib was downregulating its levels. A rapid and remarkable decrease of cyclin D1 protein levels was observed after 30 minutes of exposure to sorafenib (10  $\mu\text{mol/L}$ ) in Z-138, JEKO-1 and a representative primary MCL case (Fig. 2A). In parallel, we also found a marked downregulation of the antiapoptotic protein Mcl-1 (Fig. 2A), whose inhibition by sorafenib has been related to the blockade of protein translation (17). Consequently,

**Figure 2.** Sorafenib targeting of Mcl-1 and cyclin D1. A, Z-138, JEKO-1, and a representative MCL primary sample were incubated with 10  $\mu\text{mol/L}$  of sorafenib for the indicated times. Protein levels of cyclin D1, Mcl-1 and phosphorylation status of eIF4E were assessed by Western blotting. B, *CYCLIN D1* and *MCL-1* mRNA levels were analyzed by qRT-PCR after exposing samples (JEKO-1 and Z-138) to 10  $\mu\text{mol/L}$  sorafenib for the indicated times. *GUSB* was used as an endogenous control, and untreated cells at each time point were used as a reference control. C, MCL cells (Z-138 and JEKO-1) were treated with sorafenib (10 and 15  $\mu\text{mol/L}$ , respectively) and cycloheximide (100  $\mu\text{mol/L}$ ). Relative levels of cyclin D1 and Mcl-1 were quantified by densitometry in Western blot membranes, using  $\beta$ -actin for loading normalization. Bars represent protein stability by means of the ratio with cycloheximide/without cycloheximide. CHX, cycloheximide. D, Z-138 and JEKO-1 cells were exposed to sorafenib (10  $\mu\text{mol/L}$ ) for 6 hours, and Bax/cyclin D1 complexes were analyzed by cyclin D1 immunoprecipitation, followed by Western blot analysis of both factors.



and as translation of cyclin D1 is regulated by the activity of the translation initiator factor eIF4E (28), we examined the levels of phosphorylation of this kinase. We found that, after 30 minutes of incubation, sorafenib (10  $\mu\text{mol/L}$ ) induced a substantial decrease of phosphorylated eIF4E, both in cell lines (Z-138 and JEKO-1) and in primary cells (MCL#7; Fig. 2A).

To confirm that sorafenib was interfering with protein translation, we then checked whether this downregulation was due to transcriptional mechanisms or degradation. First, we monitored *MCL-1* and *CYCLIN D1* mRNA levels by qRT-PCR and no substantial changes either in *MCL-1* or in *CYCLIN D1* transcripts were detected after incubation of cells with 10  $\mu\text{mol/L}$  sorafenib (Fig. 2B). Next, we preincubated Z-138 and JEKO-1 cells for 4 hours with sorafenib before adding the protein synthesis inhibitor cycloheximide (100  $\mu\text{mol/L}$ ) for 1 additional hour. We found that cycloheximide addition did not enhance the decrease of cyclin D1 and Mcl-1 protein levels upon sorafenib exposure, indicating that when translation is blocked, their elimination is not increasing and therefore their stability did not diminish, even it was slightly enhanced by sorafenib (Fig. 2C).

Recently, it has been reported that cyclin D1 interacts with and sequesters the proapoptotic protein Bax in MCL cells (29). In this context, we analyzed by cyclin D1 immunoprecipitation whether Bax/cyclin D1 interaction was modulated after 6 hours of sorafenib (10  $\mu\text{mol/L}$ ) treatment in MCL cells. In the 2 representative cell lines (Z-138 and JEKO-1), we detected that although immunoprecipitated cyclin D1 decreased with sorafenib, the proportion of Bax interacting with cyclin D1 diminished even more, leading to Bax release from cyclin D1 (Fig. 2D).

Collectively, all these findings indicate that sorafenib inhibits translation of cyclin D1 and Mcl-1 as well as releases Bax from cyclin D1 sequestering in MCL cells, suggesting that both facilitate apoptosis induction.

### Sorafenib-induced apoptosis is mediated by caspase-dependent and -independent mechanisms

To further characterize the cell death mechanism of sorafenib-induced cytotoxicity, we analyzed several markers of the mitochondrial apoptotic pathway in MCL cells. As displayed in Fig. 3A, sorafenib induced Bax and Bak conformational changes, loss of  $\Delta\psi\text{m}$  and caspase-3 processing along with PS exposure, both in JEKO-1 and in a representative primary MCL (MCL#7). Next, to assess the contribution of caspases to this process, JEKO-1 and 4 primary MCL cases were preincubated for 1 hour with the pan-caspase inhibitor Q-VD-OPh (10  $\mu\text{mol/L}$ ) before sorafenib addition. Q-VD-OPh did not completely abrogate PS exposure, either in JEKO-1 or in primary cells (Fig. 3B). In consequence, sorafenib-induced apoptosis was significantly reduced ( $P < 0.05$ ) in the presence of Q-VD-OPh, but significant cell death was still detectable ( $P < 0.05$ ), indicating that caspase-independent mechanisms were also involved in its effect. On the basis of these results, we checked the cytosolic release of the caspase-

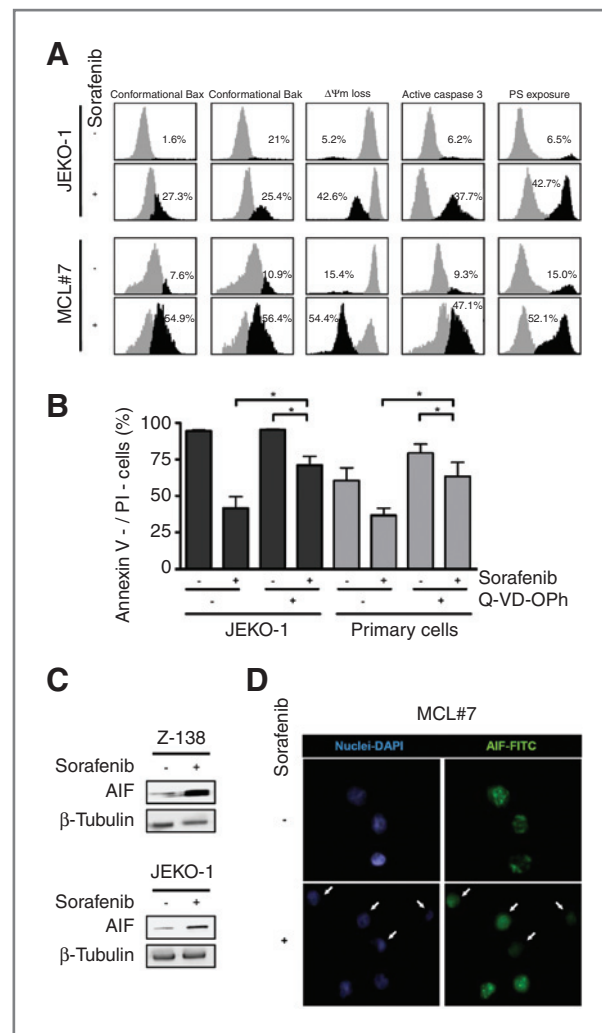


**Figure 3.** Apoptosis induction by sorafenib. A, JEKO-1 and primary cells from a representative MCL sample were exposed to sorafenib (15 and 10  $\mu\text{mol/L}$ , respectively) for 24 hours. Bax/Bak conformational changes, loss of  $\Delta\psi\text{m}$ , caspase-3 activation, and PS residues exposure were determined by flow cytometry. The percentages inside each chart refer to the population in black. B, cells were preincubated for 1 hour with Q-VD-OPh (10  $\mu\text{mol/L}$ ) followed by 24-hour exposure to sorafenib (10 or 15  $\mu\text{mol/L}$  for primary cells and JEKO-1, respectively). Cell viability was analyzed by Annexin V/PI staining. Bars represent the mean  $\pm$  SD of triplicate experiments for JEKO-1 and the mean  $\pm$  SEM of the 4 cases analyzed for primary cells. \*,  $P < 0.05$ . C, Western blot evaluation of AIF in cytosolic protein extracts from Z-138 and JEKO-1 cells exposed to sorafenib (10 and 15  $\mu\text{mol/L}$ , respectively) for 24 hours. D, a representative primary MCL sample was incubated with sorafenib (10  $\mu\text{mol/L}$ ) for 24 hours. Cells were stained for AIF-FITC (green) mounted in Fluoroshield with DAPI (blue) medium and visualized on a Eclipse 50i microscope by means of a 100 $\times$ /1.30 NA oil objective using the Isis Imaging System v5.3 software. Bars indicate the cells with release of AIF and the corresponding nuclei of a representative field.

independent apoptogenic factor AIF after sorafenib exposure. Z-138 and JEKO-1 cells were exposed to sorafenib (10 and 15  $\mu\text{mol/L}$ , respectively) for 24 hours, and pellets were processed to isolate mitochondria from cytosol. Western blot analysis in Fig. 3C showed that sorafenib

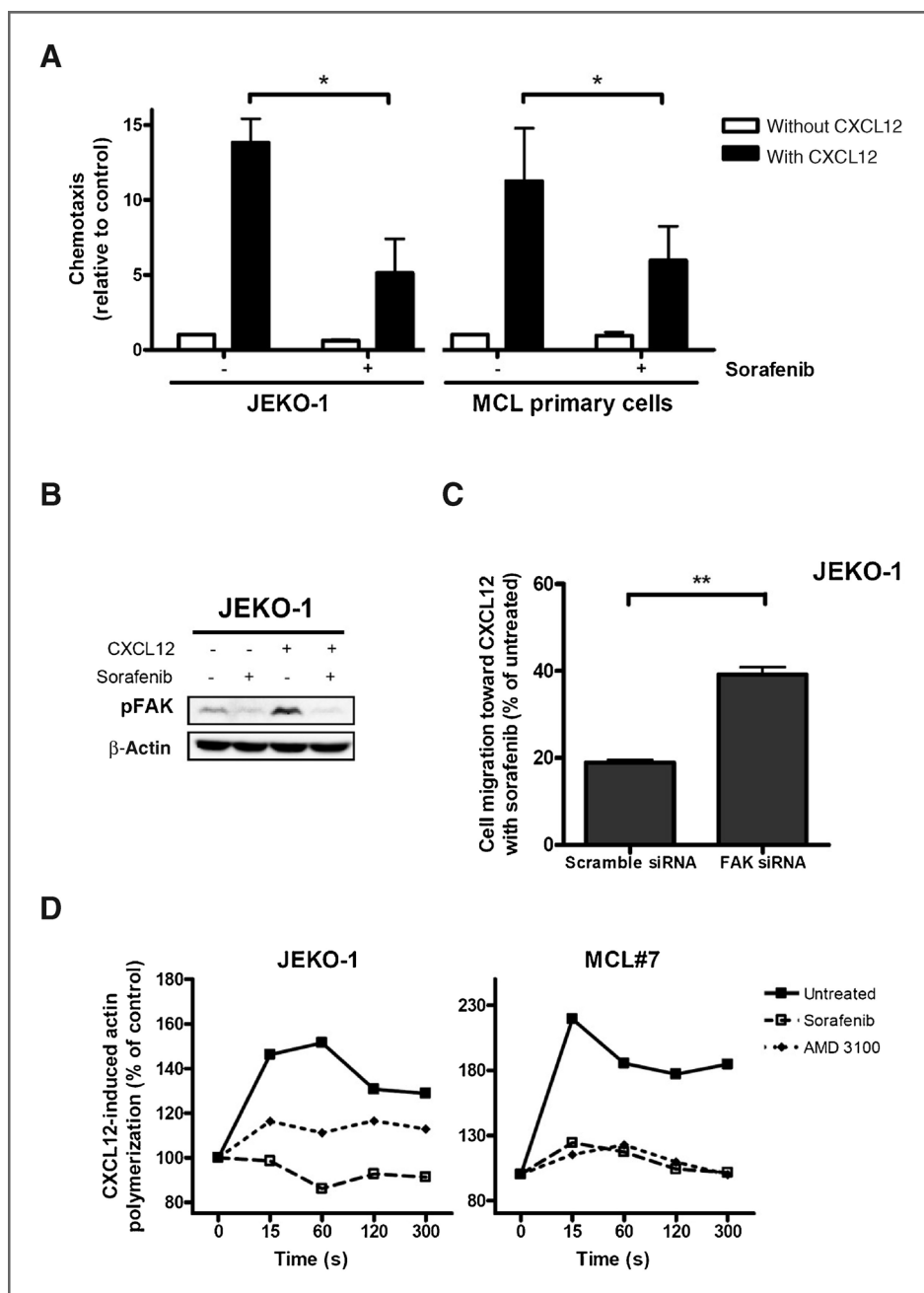
stimulated an increase of AIF in the cytosolic fraction. Consistently, immunofluorescence staining of a representative primary MCL incubated with sorafenib (10  $\mu\text{mol/L}$ ) for 24 hours showed a diffuse pattern of AIF (arrows; Fig. 3D), indicative of the cytosolic release. In contrast, untreated cells showed a punctuated pattern due to its mitochondrial localization, supporting a role of AIF in sorafenib-induced apoptotic signaling.

Together, all these data indicate that sorafenib-induced mitochondrial apoptosis is mediated by caspase-dependent and -independent mechanisms.

### Sorafenib blocks CXCL12-induced MCL migration and actin polymerization through FAK modulation

Given that FAK was rapidly inhibited by sorafenib, we next evaluated the effects of this compound on the migratory capacity of MCL cells induced by the chemokine CXCL12. As shown in Fig. 4A, sorafenib significantly reduced JEKO-1 cell migration induced by CXCL12 ( $P < 0.05$ ). To validate these results in primary samples, cells from 8 representative MCL cases were also assayed for migration as above. In all samples, sorafenib significantly blocked CXCL12-induced migration ( $P < 0.05$ ; Fig. 4A).

**Figure 4.** Chemotaxis and actin polymerization blockade by sorafenib. **A**, JEKO-1 and primary MCL cells were assayed for chemotaxis toward CXCL12 (200 ng/mL) after 1.5 hours of sorafenib (10 or 15  $\mu\text{mol/L}$  for primary cells and JEKO-1, respectively) preincubation. Bars represent the chemotaxis relative to untreated cells without CXCL12 (mean  $\pm$  SD of 3 experiments in JEKO-1, left; mean  $\pm$  SEM of 8 primary cases, right). \*,  $P < 0.05$ . **B**, Western blot analysis of phosphorylated FAK in JEKO-1 cells after preincubation with sorafenib (15  $\mu\text{mol/L}$ ) for 1 hour followed by CXCL12 stimulation (30 minutes, 200 ng/mL). **C**, FAK was silenced with an siRNA-mediated approach in JEKO-1 cells before they were assayed for chemotaxis toward CXCL12 (200 ng/mL). Bars represent mean  $\pm$  SD cell migration toward CXCL12 with sorafenib and are relative to untreated controls (100%). \*\*,  $P < 0.01$ . **D**, JEKO-1 and primary MCL cells were exposed to sorafenib (15 or 10  $\mu\text{mol/L}$ , respectively) or AMD3100 (40  $\mu\text{mol/L}$ ) for 1.5 hours. F-Actin content was determined as described in Materials and Methods at the indicated time points after CXCL12 (200 ng/mL) addition. Results are displayed relative to samples before chemokine stimulation (100%).



Accordingly, Western blot analysis revealed that sorafenib was able to abrogate CXCL12-induced phosphorylation of FAK in JEKO-1 (Fig. 4B).

To determine whether the disruption of FAK activation was functionally relevant for the antimigratory effect of sorafenib, we used an siRNA-mediated approach to knock-down FAK in JEKO-1 cells. Transfection with siRNA oligonucleotides directed against FAK gene reduced its mRNA expression by 20% (data not shown) and significantly impaired the inhibitory effect of sorafenib on cell migration

( $P < 0.01$ ; Fig. 4C). The percentage of migrating cells toward CXCL12 in the presence of sorafenib was about 19% with scramble siRNA, whereas this percentage increased to 40% with FAK siRNA (Fig. 4C). These data show that the modulation of FAK plays a pivotal role in the antimigratory activity of sorafenib in MCL cells.

One of the earliest events in the MCL migratory response to CXCL12 is the reorganization of the actin cytoskeleton (10). In this context, we evaluated whether this response could be blocked by sorafenib. CXCL12 induced a notable

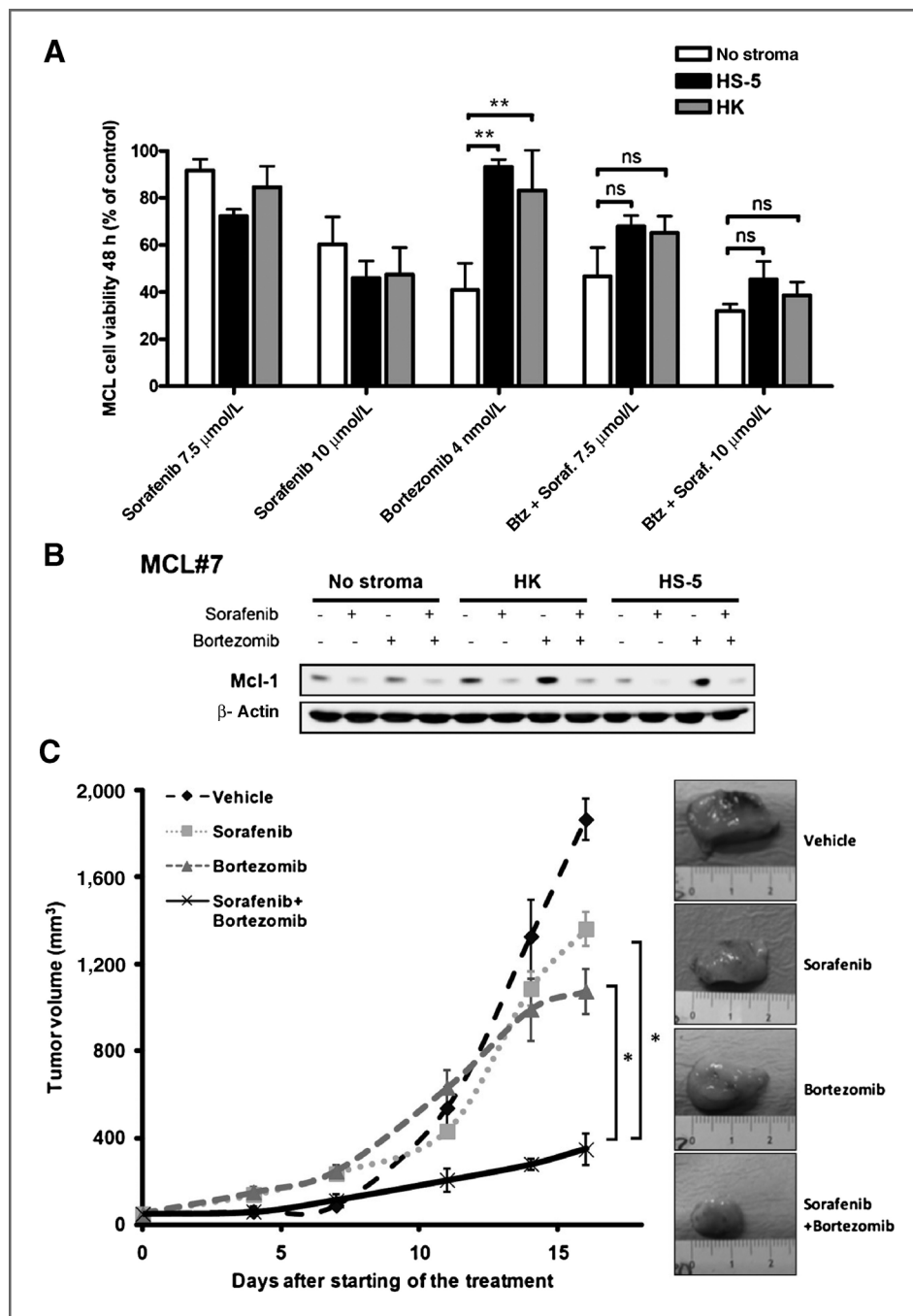


**Figure 5.** Stroma-mediated bortezomib resistance overcome by sorafenib. **A**, primary MCL cells ( $n = 5$ ) were cocultured with or without either HK or HS-5 and preincubated with sorafenib (7.5 or 10  $\mu\text{mol/L}$ ) for 1 hour before bortezomib (4 nmol/L) addition for further 48 hours. Bars represent mean  $\pm$  SEM cell viability of all the samples analyzed. ns, not significant; \*\*,  $P < 0.01$ . Btz, bortezomib; Soraf., sorafenib. **B**, Mcl-1 protein levels were analyzed by Western blotting after coculture of primary MCL cells with or without stroma and preincubation with sorafenib (10  $\mu\text{mol/L}$ ) for 1 hour before bortezomib (4 nmol/L) addition for 6 hours. **C**, JEKO-1 cells ( $10^7$  cells per mouse) were subcutaneously inoculated into the right flank of CB17-SCID mice. Tumor-bearing mice received oral sorafenib (80 mg/kg) 5 d/wk and/or intraperitoneal injections of 0.3 mg/kg bortezomib twice a week. Tumor growth is represented as the mean  $\pm$  SEM ( $n = 4$ ). \*,  $P < 0.05$ .

increase in F-actin polymerization that peaks at 15 seconds of stimulation, both in JEKO-1 (Fig. 4D) and in a representative MCL primary case (Fig. 4D). Interestingly, preincubation of MCL cells for 1.5 hours with sorafenib strongly inhibited the actin polymerization induced by CXCL12 at all time points analyzed (Fig. 4D), sorafenib being as effective as the CXCR4 antagonist AMD3100, used as a positive control of inhibition.

### Stroma-induced bortezomib resistance is overcome by sorafenib

We have recently reported that sorafenib is able to overcome the stroma-mediated resistance to common cytotoxic drugs in CLL cells (20). Therefore, we evaluated whether sorafenib could also resensitize MCL cells to bortezomib-induced apoptosis in stroma cocultures. The follicular dendritic cell-like line HK and the bone marrow-derived stromal cell line HS-5 were used to simulate the lymphoma microenvironment. Figure 5A displayed the cytotoxic effect of bortezomib (4 nmol/L) at 48 hours with or without pretreatment with sorafenib (7.5 and 10  $\mu$ mol/L) for 1 hour, in a set of 5 primary MCL cells cocultured with HS-5 and HK cells. The presence of both HS-5 and HK completely abrogated bortezomib cytotoxicity in MCL cells (\*\*; HK:  $P < 0.01$ ; HS-5:  $P < 0.01$ ). Noteworthy, the relative viability of primary MCL cells exposed to bortezomib in combination with sorafenib (7.5 and 10  $\mu$ mol/L) resulted in no significant changes with and without stroma, both in HK and in HS-5 cocultures (Fig. 5A). On the basis of these results, we further analyzed the molecular mechanisms underlying this effect. We observed that in the presence of stroma, primary MCL cells exposed to bortezomib upregulated Mcl-1 protein levels (Fig. 5B). Interestingly, 10  $\mu$ mol/L sorafenib was able to revert almost completely this effect, neutralizing bortezomib-induced Mcl-1 accumulation in the presence of the stroma. Next, to validate the combination of sorafenib and bortezomib *in vivo*, we inoculated JEKO-1 cells subcutaneously to CB17-SCID mice and examined the tumor growth. On day 19, when the tumor size reached 50 mm<sup>3</sup> in volume, mice were randomly assigned into 4 groups and treated as reported in the methods section. As shown in Fig. 5C, the combination of sorafenib and bortezomib achieved substantial MCL tumor regression and was significantly (\*,  $P < 0.05$ ) more effective in altering tumor growth than each drug alone. At 35 days after inoculation, animals were killed according to animal care guidelines. Tumors isolated from control and drug-treated MCL-bearing mice showed more than a 50% reduction in tumor burden in the combo-receiving group (Fig. 5C).

### Discussion

Targeting deregulated kinases has emerged as a promising strategy for the treatment of B lymphoid neoplasms. Here, we show for the first time that the multikinase inhibitor sorafenib induces dose- and time-dependent apoptosis in MCL cell lines as well as in primary cells, at the same micromolar range as described for CLL cells, which has

been shown to be selective for tumor cells and physiologically achievable *in vivo* (20).

In MCL cells, BCR-associated kinases are constitutively activated and highly expressed (6–8). In this context, we show that sorafenib induces a fast, sustained, and concomitant dephosphorylation of Syk, Lyn, and FAK, even in BCR-stimulated cells, indicating that BCR kinases are early and important targets of sorafenib in MCL, as described for CLL cells (20). In this line, we also show a strong synergism between sorafenib and the Syk inhibitor R406. The first clinical trials with this Syk inhibitor have only shown modest clinical responses in MCL (30), indicating that Syk blockage alone could not be effective enough. In this context, sorafenib might represent an advantage in front of Syk inhibitors due to its capacity of simultaneous targeting of several BCR-related kinases.

In B-lymphoma cells, Syk inhibition results in a decrease in mTOR activity, implicated in protein synthesis (31). At early incubation times, sorafenib induced a fast and remarkable decrease of cyclin D1 and the antiapoptotic Mcl-1. Our results suggest that the downregulation of both proteins is neither transcriptional nor through enhanced degradation but via translation blockade. This observation was previously described for Mcl-1 in other tumors (17, 19, 32), however, not for cyclin D1, which is highly overexpressed in MCL as a consequence of the t(11;14) translocation. One might consider this effect as a consequence of Syk inhibition, although a direct dephosphorylation of any of the mTOR pathway kinases by sorafenib cannot be ruled out.

The role of Mcl-1 as an antiapoptotic protein is well known (33). Accordingly, sorafenib-induced Mcl-1 downregulation may be directly impairing antiapoptotic signals, therefore committing cells to die. Less known is the involvement of cyclin D1 in apoptosis. Recently, it has been shown that cyclin D1 interacts with and sequesters the proapoptotic protein Bax in MCL cells (29). Our results indicate that sorafenib, besides decreasing cyclin D1 levels, is also disrupting this interaction and releases Bax from cyclin D1. Consequently, downregulation of both Mcl-1 and cyclin D1 as well as Bax liberation from cyclin D1 sequestering may participate in sorafenib-induced apoptosis. Furthermore, we show for the first time that sorafenib causes apoptosis in MCL through activation of the mitochondrial apoptotic pathway, leading to the activation of caspase-dependent and -independent mechanisms. As reported for other tumors (19, 34), we observed a release of AIF after sorafenib treatment pointing out the relevance of this apoptogenic factor in the cytotoxic activity of sorafenib and other anti-tumor agents in B lymphoid neoplasms (35, 36).

In addition to apoptosis induction, sorafenib is also modulating the microenvironmental interactions of MCL cells. Here, we provide the first evidence that sorafenib blocks CXCL12-induced migration and actin polymerization in both primary MCL cells and cell lines. We postulate that sorafenib, via FAK inhibition, is preventing this effect. As we reported for CLL (20), FAK is also activated after BCR engagement in MCL cells and sorafenib reverted this effect. Our data provide conclusive evidences about the role of FAK

in modulating tumor B-cell migration, as we show that *FAK* knockdown in MCL cells has a functional effect on the antimigratory properties of sorafenib. The tyrosine kinase activity of *FAK* may be both directly inhibited by sorafenib and through an *Src*-dependent mechanism, given that sorafenib is inhibiting BCR kinases. The resulting *Src/FAK* complex affects multiple proteins, such as actin cytoskeletal proteins (12). Consequently, we show a substantial blockade of cytoskeletal reorganization by sorafenib in CXCL12-stimulated MCL cells. As *FAK* may play a key role in MCL tissue microenvironments regulating the early dissemination of the tumor, sorafenib could be highly effective in overcoming this effect.

Emphasizing the role that sorafenib has in overcoming microenvironmental interactions (37), we show for the first time that the compound blocks stroma-mediated chemoresistance in MCL. Despite the approval of bortezomib in the treatment of patients with MCL, more than 50% of the patients are resistant to this therapy or show early relapses (2). One of the contributory mechanisms to bortezomib resistance is the crosstalk between MCL cells and stromal cells in tissue microenvironments (9). In this context, we have showed that in the presence of the stroma, MCL cells become resistant to bortezomib and that sorafenib overcomes this resistance. Supporting this combination, we show that in the *in vivo* setting, sorafenib plus bortezomib is more effective in reducing tumor growth than each drug alone.

Collectively, our results provide a novel mechanism of action of the multikinase inhibitor sorafenib in MCL cells, establishing that sorafenib interferes with BCR signaling, protein translation and modulates the migratory and microenvironmental prosurvival signals in MCL. These results suggest that sorafenib alone or in combination with bortezomib-based therapies may represent a promising approach to treat patients with MCL.

## References

- Jares P, Colomer D, Campo E. Genetic and molecular pathogenesis of mantle cell lymphoma: perspectives for new targeted therapeutics. *Nat Rev Cancer* 2007;7:750–62.
- Diefenbach CS, O'Connor OA. Mantle cell lymphoma in relapse: the role of emerging new drugs. *Curr Opin Oncol* 2010;22:419–23.
- Perez-Galan P, Dreyling M, Wiestner A. Mantle cell lymphoma: biology, pathogenesis, and the molecular basis of treatment in the genomic era. *Blood* 2011;117:26–38.
- Fowler N, Sharman JP, Smith SM, Boyd T, Grant B, Kolibaba KS, et al. The Btk inhibitor, PCI-32765, induces durable responses with minimal toxicity in patients with relapsed/refractory B-cell malignancies: results from a phase I study. *Blood* 2010;116:425.
- Flinn IW, Byrd JC, Furman RR, Brown JR, Benson DM, Coutre SV, et al. Evidence of clinical activity in a phase 1 study of CAL-101, an oral P110δ isoform-selective inhibitor of phosphatidylinositol 3-kinase, in patients with relapsed or refractory B-cell malignancies. *Blood* 2009;114:922.
- Boyd RS, Jukes-Jones R, Walewska R, Brown D, Dyer MJ, Cain K. Protein profiling of plasma membranes defines aberrant signaling pathways in mantle cell lymphoma. *Mol Cell Proteomics* 2009;8:1501–15.
- Rinaldi A, Kwee I, Taborelli M, Largo C, Uccella S, Martin V, et al. Genomic and expression profiling identifies the B-cell associated

## Disclosure of Potential Conflicts of Interest

No potential conflicts of interest were disclosed.

## Authors' Contributions

**Conception and design:** S. Xargay-Torrent, M. López-Guerra, D. Colomer  
**Development of methodology:** S. Xargay-Torrent, M. López-Guerra, I. Saborit-Villarroya, L. Rosich

**Acquisition of data (provided animals, acquired and managed patients, provided facilities, etc.):** S. Xargay-Torrent, M. López-Guerra

**Analysis and interpretation of data (e.g., statistical analysis, biostatistics, computational analysis):** S. Xargay-Torrent, M. López-Guerra, A. Monraveta, L. Rosich, A. Navarro

**Writing, review, and/or revision of the manuscript:** S. Xargay-Torrent, M. López-Guerra, A. Monraveta, P. Pérez-Galán, G. Roué, E. Campo, D. Colomer

**Study supervision:** E. Campo, D. Colomer

## Acknowledgments

The authors thank Laura Jiménez, Jocabed Roldán, Sandra Cabezas, and Vanina Rodríguez for their technical support. This work was carried out at the Esther Koplowitz Center, Barcelona. Sorafenib and bortezomib were kindly provided by Bayer and Millenium Pharmaceuticals, respectively.

## Grant Support

The study was supported by Ministerio de Ciencia e Innovación (SAF 09/9503), Redes Temáticas de Investigación Cooperativa de Cáncer from the Instituto de Salud Carlos III RED 2006-20-014 (D. Colomer) and 2006-20-039 (E. Campo), Fondo de Investigación Sanitaria (CP07/00072 and PI09/00060;G. Roué), and Generalitat Catalunya 2009SGR967 (D. Colomer). P. Pérez-Galán holds a contract from Ramón y Cajal program (Ministerio de Ciencia e Innovación, RYC2009-05134). S. Xargay-Torrent, L. Rosich, and A. Monraveta are recipients of predoctoral fellowships from Ministerio de Ciencia e Innovación (FPU), IDIBAPS and Ministerio de Ciencia e Innovación (FPI), respectively. M. López-Guerra and I. Saborit-Villarroya have a contract from Fundación Científica de la Asociación Española contra el Cáncer and RED 2006-20-039, respectively.

The costs of publication of this article were defrayed in part by the payment of page charges. This article must therefore be hereby marked *advertisement* in accordance with 18 U.S.C. Section 1734 solely to indicate this fact.

Received June 12, 2012; revised November 7, 2012; accepted November 28, 2012; published OnlineFirst December 11, 2012.

- tyrosine kinase Syk as a possible therapeutic target in mantle cell lymphoma. *Br J Haematol* 2006;132:303–16.
- Pighi C, Gu TL, Dalai I, Barbi S, Parolini C, Bertolaso A, et al. Phosphoproteomic analysis of mantle cell lymphoma cells suggests a prosurvival role of B-cell receptor signaling. *Cell Oncol (Dordr)* 2011;34:141–53.
- Burger JA, Ford RJ. The microenvironment in mantle cell lymphoma: cellular and molecular pathways and emerging targeted therapies. *Semin Cancer Biol* 2011;21:308–12.
- Kurtova AV, Tamayo AT, Ford RJ, Burger JA. Mantle cell lymphoma cells express high levels of CXCR4, CXCR5, and VLA-4 (CD49d): importance for interactions with the stromal microenvironment and specific targeting. *Blood* 2009;113:4604–13.
- Brunton VG, Frame MC. *Src* and focal adhesion kinase as therapeutic targets in cancer. *Curr Opin Pharmacol* 2008;8:427–32.
- Kim LC, Song L, Haura EB. *Src* kinases as therapeutic targets for cancer. *Nat Rev Clin Oncol* 2009;6:587–95.
- Escudier B, Eisen T, Stadler WM, Szczylik C, Oudard S, Siebels M, et al. Sorafenib in advanced clear-cell renal-cell carcinoma. *N Engl J Med* 2007;356:125–34.
- Llovet JM, Ricci S, Mazzaferro V, Hilgard P, Gane E, Blanc JF, et al. Sorafenib in advanced hepatocellular carcinoma. *N Engl J Med* 2008;359:378–90.

15. Kurosu T, Ohki M, Wu N, Kagechika H, Miura O. Sorafenib induces apoptosis specifically in cells expressing BCR/ABL by inhibiting its kinase activity to activate the intrinsic mitochondrial pathway. *Cancer Res* 2009;69:3927–36.
16. Auclair D, Miller D, Yatsula V, Pickett W, Carter C, Chang Y, et al. Antitumor activity of sorafenib in FLT3-driven leukemic cells. *Leukemia* 2007;21:439–45.
17. Huber S, Oelsner M, Decker T, zum Buschenfelde CM, Wagner M, Lutzny G, et al. Sorafenib induces cell death in chronic lymphocytic leukemia by translational downregulation of Mcl-1. *Leukemia* 2011;25:838–47.
18. Messmer D, Fecteau JF, O'Hayre M, Bharati IS, Handel TM, Kipps TJ. Chronic lymphocytic leukemia cells receive RAF-dependent survival signals in response to CXCL12 that are sensitive to inhibition by sorafenib. *Blood* 2011;117:882–9.
19. Rahmani M, Davis EM, Bauer C, Dent P, Grant S. Apoptosis induced by the kinase inhibitor BAY 43-9006 in human leukemia cells involves down-regulation of Mcl-1 through inhibition of translation. *J Biol Chem* 2005;280:35217–27.
20. Lopez-Guerra M, Xargay-Torrent S, Perez-Galan P, Saborit-Villarroya I, Rosich L, Villamor N, et al. Sorafenib targets BCR kinases and blocks migratory and microenvironmental survival signals in CLL cells. *Leukemia* 2012;26:1429–32.
21. Salaverria I, Perez-Galan P, Colomer D, Campo E. Mantle cell lymphoma: from pathology and molecular pathogenesis to new therapeutic perspectives. *Haematologica* 2006;91:11–6.
22. Swerdlow SH, Campo E, Harris NL, Jaffe ES, Pileri SA, Stein H, et al. WHO classification of tumours of haematopoietic and lymphoid tissues. 4th ed. Lyon, France: International Agency for Research on Cancer; 2008.
23. Bellosillo B, Villamor N, Lopez-Guillermo A, Marce S, Bosch F, Campo E, et al. Spontaneous and drug-induced apoptosis is mediated by conformational changes of Bax and Bak in B-cell chronic lymphocytic leukemia. *Blood* 2002;100:1810–6.
24. Ghia P, Stamatopoulos K, Belessi C, Moreno C, Stilgenbauer S, Stevenson F, et al. ERIC recommendations on IGHV gene mutational status analysis in chronic lymphocytic leukemia. *Leukemia* 2007;21:1–3.
25. Xargay-Torrent S, Lopez-Guerra M, Saborit-Villarroya I, Rosich L, Campo E, Roue G, et al. Vorinostat-induced apoptosis in mantle cell lymphoma is mediated by acetylation of proapoptotic BH3-only gene promoters. *Clin Cancer Res* 2011;17:3956–68.
26. Roue G, Perez-Galan P, Mozos A, Lopez-Guerra M, Xargay-Torrent S, Rosich L, et al. The Hsp90 inhibitor IPI-504 overcomes bortezomib resistance in mantle cell lymphoma in vitro and in vivo by down-regulation of the prosurvival ER chaperone BiP/Grp78. *Blood* 2011;117:1270–9.
27. Kim HS, Zhang X, Klyushnenkova E, Choi YS. Stimulation of germinal center B lymphocyte proliferation by an FDC-like cell line, HK. *J Immunol* 1995;155:1101–9.
28. Rosenwald IB, Lazaris-Karatzas A, Sonenberg N, Schmidt EV. Elevated levels of cyclin D1 protein in response to increased expression of eukaryotic initiation factor 4E. *Mol Cell Biol* 1993;13:7358–63.
29. Beltran E, Fresquet V, Martinez-Useros J, Richter-Larrea JA, Sagardoy A, Sesma I, et al. A cyclin-D1 interaction with BAX underlies its oncogenic role and potential as a therapeutic target in mantle cell lymphoma. *Proc Natl Acad Sci U S A* 2011;108:12461–6.
30. Friedberg JW, Sharman J, Sweetenham J, Johnston PB, Vose JM, Lacasce A, et al. Inhibition of Syk with fostamatinib disodium has significant clinical activity in non-Hodgkin lymphoma and chronic lymphocytic leukemia. *Blood* 2010;115:2578–85.
31. Leseux L, Hamdi SM, Al ST, Capilla F, Recher C, Laurent G, et al. Syk-dependent mTOR activation in follicular lymphoma cells. *Blood* 2006;108:4156–62.
32. Gobessi S, Laurenti L, Longo PG, Carsetti L, Bero V, Sica S, et al. Inhibition of constitutive and BCR-induced Syk activation downregulates Mcl-1 and induces apoptosis in chronic lymphocytic leukemia B cells. *Leukemia* 2009;23:686–97.
33. Quinn BA, Dash R, Azab B, Sarkar S, Das SK, Kumar S, et al. Targeting Mcl-1 for the therapy of cancer. *Expert Opin Investig Drugs* 2011;20:1397–411.
34. Panka DJ, Wang W, Atkins MB, Mier JW. The Raf inhibitor BAY 43-9006 (Sorafenib) induces caspase-independent apoptosis in melanoma cells. *Cancer Res* 2006;66:1611–9.
35. Roue G, Lopez-Guerra M, Milpied P, Perez-Galan P, Villamor N, Montserrat E, et al. Bendamustine is effective in p53-deficient B-cell neoplasms and requires oxidative stress and caspase-independent signaling. *Clin Cancer Res* 2008;14:6907–15.
36. Lopez-Guerra M, Roue G, Perez-Galan P, Alonso R, Villamor N, Montserrat E, et al. p65 activity and ZAP-70 status predict the sensitivity of chronic lymphocytic leukemia cells to the selective I $\kappa$ B kinase inhibitor BMS-345541. *Clin Cancer Res* 2009;15:2767–76.
37. Burger JA, Ghia P, Rosenwald A, Caligaris-Cappio F. The micro-environment in mature B-cell malignancies: a target for new treatment strategies. *Blood* 2009;114:3367–75.

# Clinical Cancer Research

## Sorafenib Inhibits Cell Migration and Stroma-Mediated Bortezomib Resistance by Interfering B-cell Receptor Signaling and Protein Translation in Mantle Cell Lymphoma

Sílvia Xargay-Torrent, Mónica López-Guerra, Arnau Montraveta, et al.

*Clin Cancer Res* 2013;19:586-597. Published OnlineFirst December 11, 2012.

**Updated version** Access the most recent version of this article at:  
doi:[10.1158/1078-0432.CCR-12-1935](https://doi.org/10.1158/1078-0432.CCR-12-1935)

**Cited articles** This article cites 36 articles, 19 of which you can access for free at:  
<http://clincancerres.aacrjournals.org/content/19/3/586.full#ref-list-1>

**Citing articles** This article has been cited by 3 HighWire-hosted articles. Access the articles at:  
<http://clincancerres.aacrjournals.org/content/19/3/586.full#related-urls>

**E-mail alerts** [Sign up to receive free email-alerts](#) related to this article or journal.

**Reprints and Subscriptions** To order reprints of this article or to subscribe to the journal, contact the AACR Publications Department at [pubs@aacr.org](mailto:pubs@aacr.org).

**Permissions** To request permission to re-use all or part of this article, use this link  
<http://clincancerres.aacrjournals.org/content/19/3/586>.  
Click on "Request Permissions" which will take you to the Copyright Clearance Center's (CCC) Rightslink site.